J Biol Inorg Chem (2007) 12:777–787
DOI 10.1007/s00775-007-0229-7

ORIGINAL PAPER

NADH oxidase activity of rat and human liver xanthine oxidoreductase: potential role in superoxide production

Luisa Maia · Rui O. Duarte · Ana Ponces-Freire · José J. G. Moura · Lurdes Mira

Received: 4 January 2007 / Accepted: 12 March 2007 / Published online: 18 April 2007

Abstract To characterise the NADH oxidase activity of both xanthine dehydrogenase (XD) and xanthine oxidase (XO) forms of rat liver xanthine oxidoreductase (XOR) and to evaluate the potential role of this mammalian enzyme as an $O_2^{\bullet-}$ source, kinetics and electron paramagnetic resonance (EPR) spectroscopic studies were performed. A steady-state kinetics study of XD showed that it catalyses NADH oxidation, leading to the formation of one $O_2^{\bullet-}$ molecule and half a H_2O_2 molecule per NADH molecule, at rates 3 times those observed for XO (29.2 ± 1.6 and 9.38 ± 0.31 min^{-1}, respectively). EPR spectra of NADH-reduced XD and XO were qualitatively similar, but they were quantitatively quite different. While NADH efficiently reduced XD, only a great excess of NADH reduced XO. In agreement with reductive titration data, the XD specificity constant for NADH (8.73 ± 1.36 μM^{-1} min^{-1}) was found to be higher than that of the XO specificity constant (1.07 ± 0.09 μM^{-1} min^{-1}). It was confirmed that, for the reducing substrate xanthine, rat liver XD is also a better $O_2^{\bullet-}$ source than XO. These data show that the dehydrogenase form of liver XOR is, thus, intrinsically more efficient at generating $O_2^{\bullet-}$ than the oxidase form, independently of the reducing substrate. Most importantly, for comparative purposes, human liver XO activity towards NADH oxidation was also studied, and the kinetics parameters obtained were found to be very similar to those of the XO form of rat liver XOR, foreseeing potential applications of rat liver XOR as a model of the human liver enzyme.

Keywords Xanthine oxidoreductase · Xanthine oxidase · Xanthine dehydrogenase · Rat liver · Reactive oxygen species · NADH

Abbreviations

AFR	Activity-to-flavin ratio
AO	Aldehyde oxidase
EPR	Electron paramagnetic resonance
FAD	Flavin adenine dinucleotide
ROS	Reactive oxygen species
Sim	Simulated
XD	Xanthine dehydrogenase
XO	Xanthine oxidase
XOR	Xanthine oxidoreductase

Introduction

Xanthine oxidoreductase (XOR), until recently also referred to as xanthine oxidase (XO), has been the subject of

L. Maia · A. Ponces-Freire · L. Mira
Centro de Química e Bioquímica,
Faculdade de Ciências da Universidade de Lisboa,
1749-016 Lisbon, Portugal

L. Maia · A. Ponces-Freire · L. Mira (✉)
Departamento de Química e Bioquímica,
Faculdade de Ciências,
Universidade de Lisboa,
1749-016 Lisbon, Portugal
e-mail: lurdes.mira@fc.ul.pt

R. O. Duarte · J. J. G. Moura
REQUIMTE/CQFB,
Departamento de Química,
Faculdade de Ciências e Tecnologia
da Universidade Nova de Lisboa,
2829-516 Caparica, Portugal

L. Mira
Centro de Metabolismo e Endocrinologia
da Faculdade de Medicina de Lisboa,
Faculdade de Medicina de Lisboa,
1649-016 Lisbon, Portugal

many mechanistic, structural and biophysical reviews [1–4]. Mammalian XOR is the key enzyme in the catabolism of purines, oxidising hypoxanthine to xanthine and xanthine to the terminal catabolite urate. XOR is a complex homodimer, containing one molybdopterin, one flavin adenine dinucleotide (FAD) and two different [2Fe–2S] centres (named Fe/S I and Fe/S II) per 145-kDa subunit [1]. The mammalian XOR is synthesised as an NAD^+-dependent dehydrogenase (throughout the text referred to as xanthine dehydrogenase, XD) but, although it transfers the electrons preferentially to NAD^+, it can also catalyse electron transfer to O_2. XD can, however, be readily converted to a ''strict'' oxidase form (named XO), either reversibly, through oxidation of the cysteine residues 535 and 992, or irreversibly, by proteolysis [5, 6]. The cysteine oxidation (or proteolysis) causes a conformational change in the vicinity of the FAD, the site at which O_2 and NAD^+ react, increasing the midpoint potential of the flavin moiety and blocking the access of NAD^+ to FAD, but without disturbing the interactions between O_2 and FAD [7].

The reduction of O_2, catalysed by both enzyme forms, yields $O_2^{\bullet-}$ and H_2O_2, with the stoichiometry of these reaction products being differentially affected by the form and the source of the enzyme and by the reactant concentrations [8, 9]. Therefore, XOR can act as a source of reactive oxygen species (ROS) and it is this capacity of XOR that makes the enzyme the focus of interest in many recent biochemical and clinical studies. Normal processes of metabolism continuously form ROS, and many of them may have useful physiological functions, such as in host defence against invading pathogens, and as mediators of signal transduction [10, 11]. Their overproduction, however, can play a major role in several pathological conditions [12–16]. Moreover, it was recently shown that XOR can catalyse the reduction of nitrates and nitrites, giving rise to both $^{\bullet}NO$ [17,18] and peroxynitrite ($ONOO^-$) [19]. This fact further amplifies the physiological and pathological significance of XOR. Unlike NO synthase, XOR can produce $^{\bullet}NO$ under anoxic conditions and, thus, promote the $^{\bullet}NO$-dependent vasodilatation in ischaemic tissues [20]. On the other hand, $ONOO^-$, a powerful oxidant and destructive agent, which results from the diffusion-controlled reaction between $^{\bullet}NO$ and $O_2^{\bullet-}$ [21], can be produced solely by the action of XOR [19]. The XOR-derived $ONOO^-$ has been proposed as a bactericidal agent in milk and the digestive tract [19].

XOR has a broad specificity for reducing substrates. In addition to the well-known oxidation of hypoxanthine and xanthine, XOR also catalyses the oxidation of a wide variety of aldehydes and substituted pyridines, purines, pteridines and related compounds, including NADH [22]. The reaction catalysed by XOR can be separated into a reductive half-reaction and an oxidative half-reaction. The reducing substrates are oxidised at the molybdenum site, and the reduction mechanism is thought to be the same for both XD and XO [1, 7]. The electrons thus transferred from the substrate to the enzyme are rapidly distributed throughout the other centres, by intramolecular electron transfer, according to their redox potentials. In the oxidative half-reaction, electrons are transferred from the FAD centre to NAD^+ or O_2 [1, 23]. NADH, although a reducing substrate, is an important exception, since electron transfer is achieved through the FAD centre [1].

The present knowledge of XOR biochemistry is mainly based on the most studied bovine milk XO and, to a lesser extent, on chicken liver XD. Several studies on bovine milk XOR and, more recently, on human milk XOR [24], which enable a direct comparison between XD and XO forms, have also been performed. In contrast, mammalian liver enzymes, with much more potential clinical relevance, have been poorly studied; it being generally accepted that they have similar kinetics and spectroscopic properties to those described for bovine milk or with avian origin. This is not necessarily correct, as it will be later discussed (see ''Discussion''). In particular, NADH oxidase activity of mammalian liver XOR has not been studied. The activity of this NADH oxidase would be of special importance in ROS-mediated diseases, such as ethanol hepatotoxicity and ischaemia-reperfusion injury, pathological states in which an increase in NADH concentration is observed [25–27] and where the generation of $O_2^{\bullet-}$ and H_2O_2 would be greatly amplified. To characterise this potential ''new'' mammalian liver ROS source, the NADH oxidase activities of both XD and XO forms of rat liver XOR were studied, with particular regard to their rates and reaction products.

To accomplish this, in the present work, rat liver XOR was successfully purified in its XO reversible form and steady-state kinetics of NADH consumption and $O_2^{\bullet-}$ production were compared between the XD and XO forms of the enzyme. In addition, electronic paramagnetic resonance (EPR) spectroscopic studies with dithionite and NADH-reduced XD and XO were performed. To emphasise the differences between milk and mammalian liver enzymes, the catalytic properties of bovine milk XO towards NADH oxidation were also studied. A parallel study was carried out with a human liver XO isoform, to compare its kinetics parameters with those obtained for the rat liver XO isoform. In addition, the NADH oxidase activity of rat liver aldehyde oxidase (AO) was also characterised. AO is structurally very similar to XOR, containing one FAD, two nonidentical [2Fe–2S] centres and one molybdopterin, in a homodimeric structure. Both enzymes have broad and overlapping specificity for reducing substrates but, unlike XOR, AO cannot be converted to a dehydrogenase form, being unable to utilise NAD^+ as the oxidising substrate [28].

Materials and methods

Adult male Sprague–Dawley rats (3–4 months old) were obtained from the Instituto de Investigação Científica Bento da Rocha Cabral (Lisbon, Portugal).

All the reagents were of the highest quality available and were used as supplied. Horse heart ferricytochrome *c*, *p*-dimethylaminocinnamaldehyde, dithiothreitol, NADH, NAD^+, xanthine, bovine milk XO and bovine erythrocytes superoxide dismutase were from Sigma Chemical Co. (Madrid, Spain). All the other reagents were from Merck (Darmstadt, Germany). NADH, NAD^+ and xanthine concentrations were determined spectrophotometrically using ε = 6,220 M^{-1} cm^{-1} at 340 nm, ε = 18,000 M^{-1} cm^{-1} at 260 nm and ε = 9,300 M^{-1} cm^{-1} at 277 nm, respectively. Activity assays and spectra were recorded using a PC-linked UV2-100 Unicam spectrophotometer with a temperature controlled cell unit.

Enzyme assays

XO activity was measured using 20 μM xanthine in 50 mM phosphate buffer pH 7.8, at 298 K, in air-equilibrated solution, with the production of urate being monitored at 295 nm (ε = 9,500 M^{-1} cm^{-1}). XD activity was measured using the same assay mixture as described for XO, plus 85 μM NAD^+ and monitoring NADH production at 340 nm (ε = 6,220 M^{-1} cm^{-1}). One unit of catalytic activity is defined as the amount of enzyme required to catalyse the oxidation of 1 μmol min^{-1} of substrate, under our experimental conditions. The dehydrogenase-to-oxidase ratio of XOR, as defined by Waud and Rajagopalan [29], was determined as the ratio of aerobic formation of urate, measured at 295 nm, in the presence of NAD^+ to that in the absence of NAD^+. AO activity was assayed by following the oxidation of 25 μM *p*-dimethylaminocinnamaldehyde at 398 nm (ε = 30,500 M^{-1} cm^{-1}) in 50 mM phosphate buffer pH 7.8, at 298 K, in air-equilibrated solution.

Purification of the XO form of XOR and AO from rat liver

XOR, in its reversible XO form, and AO were purified from rat liver as previously described by Maia and Mira [30]. Briefly, the rat liver homogenate was fractionated by heat denaturation and by ammonium sulfate precipitation to give a crude extract containing both enzymes. This extract was chromatographed on a hydroxyapatite column (Bio-Rad, CA, USA) that completely separated AO from XO. Further purification of XO forms by anion-exchange chromatography on a Q-Sepharose Fast Flow column (Pharmacia Biotech, Uppsala, Sweden) resulted in a highly purified (about 1,200-fold) preparation, with a specific activity of 3.5–3.7 U mg^{-1}. AO was purified about 1,000-fold, with a specific activity of 3.4–3.6 U mg^{-1}, by affinity chromatography on benzamidine-Sepharose 6B (Pharmacia Biotech, Uppsala, Sweden). Both purified enzymes displayed the characteristic absorption spectra of highly purified enzymes, with absorbance ratios Abs_{280}/Abs_{450} between 5.3 and 5.8. To evaluate the presence of inactive forms of the enzyme (desulfo and demolybdo), the activity-to-flavin ratio (AFR) of the XO form was calculated, dividing the absorbance change per minute at 295 nm by the absorbance at 450 nm of the enzyme used in the assay (200 was taken to be 100% active [31]). The final XO concentration was determined spectrophotometrically using ε = 71,500 M^{-1} cm^{-1} at 450 nm for the oxidised enzyme [32], and was corrected for the presence of inactive molecules. The XO batches thus obtained did not have xanthine:NAD^+ oxidoreductase activity.

Preparation of the dehydrogenase form of XOR from rat liver

XOR in its XD form was obtained through reversible reduction of oxidised XO sulfhydryl groups. Purified XO was incubated with 5 mM dithiothreitol, for 1–2 h, at 303 K, and then passed through a small G-25 column (Pharmacia Biotech, Uppsala, Sweden) equilibrated in 100 mM tris(hydroxymethyl)aminomethane (Tris)–HCl buffer, pH 7.8. Dithiothreitol treatment resulted in an 80–85% decrease in the XO activity (xanthine:O_2 oxidoreductase activity) and a dehydrogenase-to-oxidase ratio of 5–6 was achieved, as previously described [30]. Considering the intrinsic xanthine:O_2 oxidoreductase activity of the XD form [31, 33, 34], the XD batches thus prepared are highly purified, with less than 5% irreversible XO contamination.

Preparation of the deflavo-XD form of XOR

THe deflavo-XD form of XOR was prepared as described by Branzoli and Massey [35].

Preparation of XO from butter milk

Lyophilised XO from butter milk, obtained from Sigma Chemical Co. (Madrid, Spain), was desalted by gel filtration on a small G-25 column (Pharmacia Biotech, Uppsala, Sweden) equilibrated in 100 mM Tris–HCl buffer, pH 7.8.

Purification of the XO form of XOR from human liver

XO was prepared from one sample (38 g) of human liver (4 days after death), as described earlier for rat liver XO.

However, the resulting enzyme sample displayed a comparatively low Abs_{280}/Abs_{450} of 9.5.

Steady-state kinetics of NADH oxidation by XOR

The initial rates of NADH oxidation by both XD and XO forms of XOR were measured following the decrease in absorbance at 340 nm (ε = 6,220 M^{-1} cm^{-1}). The enzymes were incubated with varying concentrations of NADH (2.5–100 μM) in air-equilibrated 50 mM Tris–HCl buffer, with 1 mM EDTA, pH 7.8. Each initial rate determination was performed with three different enzyme batches, in quintuplicate, except for bovine milk XO, for which only one enzyme lot was assayed. The apparent kinetics parameters were estimated by the direct linear method of Eisenthal and Cornish-Bowden [36]. The values obtained using the double-reciprocal plot agreed within a maximum error of 7%. The specificity constants were calculated as $k_{NADH} = k_{cat}^{app}/K_m^{app}$.

Steady-state kinetics of $O_2^{\bullet-}$ formation by XOR

$O_2^{\bullet-}$ formation during NADH oxidation by both XD and XO forms of XOR was estimated as the superoxide dismutase inhibitable reduction of cytochrome *c* [37]. The reaction mixtures contained 50 mM Tris–HCl buffer, with 1 mM EDTA, pH 7.8, 100 μM ferricytochrome *c* and varying concentrations of NADH (2.5–100 μM). The initial rates of $O_2^{\bullet-}$ formation (determined in quintuplicate and with three different enzyme batches) were evaluated by the increase in absorbance at 550 nm ($\Delta\varepsilon$ = 21,000 M^{-1} cm^{-1}) in the absence and in the presence of 2,500 U cm^{-3} superoxide dismutase. The apparent kinetics parameters were estimated by the direct linear method of Eisenthal and Cornish-Bowden [36]. The values obtained using the double-reciprocal plot agreed within a maximum error of 3%. The specificity constants were calculated as $k_{NADH} = k_{cat}^{app}/K_m^{app}$.

One-electron reduction flux

The percentage of oxygen one-electron reduction was calculated as half of the ratio of the $O_2^{\bullet-}$ production rate to the NADH oxidation rate, with the initial rates being calculated from the kinetics parameters determined.

Reductive titration of rat liver XOR and the deflavo-XD form

Reductive titrations of both the XD and XO forms of rat liver XOR with NADH were followed by EPR spectroscopy at 20, 40, 60 and 100 K. The enzyme samples were reduced anaerobically with NADH for 5 min in 50 mM Tris–HCl buffer pH 7.8 at 293 K before being frozen. Enzymes were also reduced with dithionite, for 30 min. The samples were cooled with an Oxford Instruments ESR900 liquid-helium cryostat, fitted with a temperature controller. X-band EPR spectra were recorded using a Bruker EMX 6/1 spectrometer, equipped with a dual-mode ER4116DM cavity. The experimental conditions maintained an amplitude and a frequency of modulation of 0.405 mT and 100 kHz, respectively, 0.0635-mW microwave power and a signal gain of 2.00×10^5 (with NADH) or 2.00×10^4 (with dithionite). EPR spectra are presented as the first derivative of absorption, in arbitrary units, and g_1, g_2 and g_3 factors stand for the low-field, medium-field and high-field lines.

The $FADH^{\bullet}$, Mo(V), Fe/S I and Fe/S II EPR signals were simulated individually with the SimFonia program from Bruker and, subsequently, added together in different proportions, until a good agreement between the simulated and the experimental spectrum was observed. Spin quantifications of the EPR signals were determined by double integration of the first derivative of the spectra relative to the spectrum of Cu^{2+}-EDTA (3 mM), recorded under nonsaturating conditions.

Results

Steady-state kinetics of NADH oxidation catalysed by rat liver XOR

NADH oxidation, catalysed by both XD and XO forms of rat liver XOR, was studied by following the disappearance of NADH spectrophotometrically at 340 nm, in air-equilibrated buffer at 298 K. The initial rates, measured at different NADH concentrations, are shown in Fig. 1. No substrate inhibition was observed, and the experimental data fitted well to the Michaelis–Menten equation, giving the apparent kinetics parameters presented in Table 1. NADH is a significantly better substrate for XD, with a higher k_{cat}^{app} and a lower K_m^{app}, than XO. Similar assays were performed in the presence of 50, 200 and 550 μM allopurinol (a XOR inhibitor, which acts at the molybdenum centre) and with enzyme batches with low AFR (73 and 96). Reaction profiles, identical to those of noninhibited and 100% active enzymes, were obtained in all cases. NADH oxidation was not observed in the presence of deflavo-XD, confirming that NADH oxidation by XD occurs at its flavin centre.

NADH oxidation catalysed by rat liver AO was also studied spectrophotometrically and fluorimetrically, but the oxidation rates were much slower, to enable accurate value determinations.

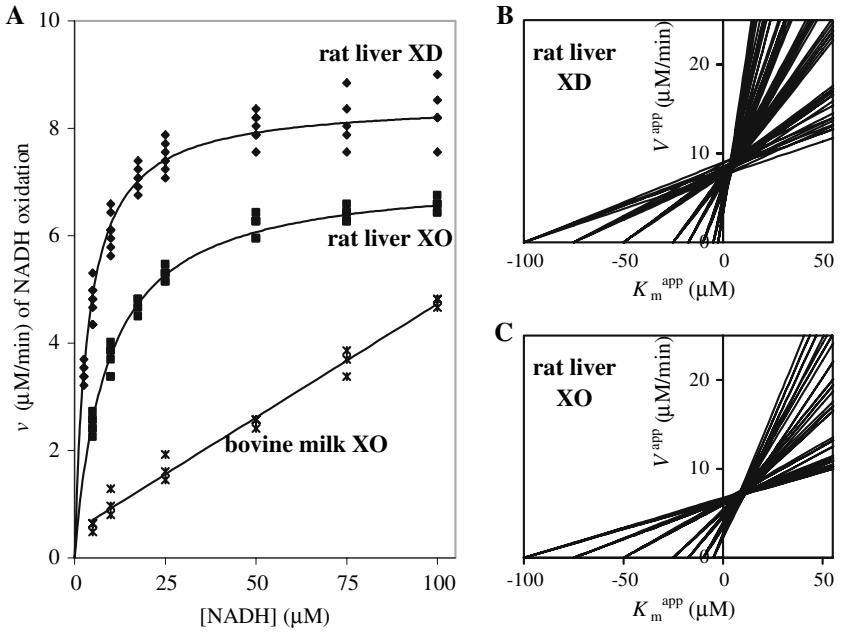

Fig. 1 NADH oxidation catalysed by both xanthine dehydrogenase (*XD*) and xanthine oxidase (*XO*) forms of rat liver xanthine oxidoreductase (XOR) and by bovine milk XO. Initial rates of NADH oxidation, catalysed by rat liver XD (0.275 μM) and XO (0.750 μM) forms and by bovine milk XO (0.750 μM), were measured spectrophotometrically at 340 nm, in air-equilibrated tris(hydroxymethyl)aminimethane (Tris)–HCl 50 mM buffer pH 7.8. **a** The values represented for the rat liver XD and XO were from a representative experiment and the *hyperbolic curves* were generated with the apparent kinetics parameters given in Table 1 and estimated by the direct linear plots shown in **b** and **c**

Table 1 Kinetics parameters (catalytic, Michaelis–Menten and specificity constants) for NADH oxidation and $O_2^{\bullet-}$ formation

Enzyme	k_{cat}^{app} (min^{-1})	K_m^{app} (μM)	k_{NADH} (μM^{-1} min^{-1})
For NADH oxidation			
XD (rat liver)	29.2 ± 1.6	3.34 ± 0.34	8.73 ± 1.36
XO (bovine milk)	Deviation from saturation kinetics		
XO (rat liver)	9.38 ± 0.31	8.73 ± 0.44	1.07 ± 0.09
For $O_2^{\bullet-}$ formation			
XD (rat liver)	27.4 ± 1.0	3.27 ± 0.16	8.40 ± 0.73
XO (rat liver)	9.20 ± 0.18	8.40 ± 0.26	1.10 ± 0.06
AO (rat liver)	2.63 ± 0.30	5.13 ± 0.38	0.512 ± 0.096

The values shown are means (± standard deviation) of three independent experiments performed with three different enzyme batches
AO aldehyde oxidase, *XD* xanthine dehydrogenase, *XO* xanthine oxidase

Steady-state kinetics of NADH oxidation catalysed by bovine milk XO

For comparative purposes, NADH oxidation catalysed by bovine milk XO was also studied and the initial rates for different NADH concentrations were determined (Fig. 1). To emphasise the differences in the kinetics between the rat liver and the bovine milk enzymes, the rat liver XO and XD data were fitted to hyperbolic curves, while the bovine milk XO data presented were fitted to a straight line. As can be observed, although the bovine milk XO showed no saturation kinetics, the rat liver XO and XD forms are better catalysts for NADH oxidation than the bovine milk XO, in particular at lower and physiologically more important NADH concentrations.

Steady-state kinetics of NADH oxidation catalysed by human liver XO

NADH oxidation catalysed by human liver XO was studied with an enzyme batch presenting a purification degree lower than the ones recovered from rat liver. The apparent values of K_m (7.5 μM) and V (5.3 μM min^{-1}) were determined by fitting the data to the Michaelis–Menten equation

(Fig. 2). A $k_{cat}^{app} \geq 13$ min^{-1} was estimated, taking into account an XO concentration lower than 0.40 μM (ε_{450nm} = 71,500 M^{-1} cm^{-1}) [32]. The human and rat liver XO specificity constants for NADH are, therefore, of the same magnitude: 1.73 and 1.07 μM^{-1} min^{-1}, respectively.

Steady-state kinetics of $O_2^{\bullet-}$ formation during NADH oxidation catalysed by rat liver XOR

During NADH oxidation catalysed by both XD and XO forms of rat liver XOR, O_2 is reduced to $O_2^{\bullet-}$ and H_2O_2. The $O_2^{\bullet-}$ formation, estimated as the superoxide dismutase inhibitable reduction of cytochrome *c*, followed saturation kinetics with no evidence of substrate inhibition (for 2.5–100 μM NADH). The initial rates of $O_2^{\bullet-}$ generation were fitted to a Michaelis–Menten equation and the calculated apparent kinetics parameters are shown in Table 1. Similarly, it was observed that when NADH oxidation was followed, the XD specificity constant for NADH was higher (8.40 ± 0.73 μM^{-1} min^{-1}) than that obtained for XO (1.10 ± 0.06 μM^{-1} min^{-1}). Accordingly, these results show that the XD form is intrinsically more efficient at generating $O_2^{\bullet-}$ than the XO form of XOR. It is important to note that the values of the XO and XD kinetics constants for NADH, determined via $O_2^{\bullet-}$ production, were close to those obtained via NADH oxidation. These results indicate that, when the reductive substrate is NADH, the fraction of $O_2^{\bullet-}/H_2O_2$ formed does not depend on its concentration. This became evident when the percentages of oxygen one-electron reductions were calculated and found to be approximately constant for any NADH concentration (Fig. 3). These results must be emphasised, since they contradict those obtained for the bovine milk XO during xanthine oxidation, in which the percentage of $O_2^{\bullet-}$ generated decreases (25–35%) as the concentration of xanthine increases [8, 9].

EPR spectral properties of reduced rat liver XOR

Since each of the redox centres of XOR is paramagnetic in one of its oxidation states, the reduction profiles of FADH$^{\bullet}$, Mo(V) and reduced Fe/S centres may be studied by EPR spectroscopy [38]. To characterise the EPR signals of redox centres of XD and XO forms of rat liver XOR, the purified enzymes were reduced with an excess of dithionite for 30 min, and the X-band EPR spectra were acquired at different temperatures (20–100 K). The EPR spectra of the dithionite-reduced XD form (Fig. 4) and XO form (not shown) were qualitatively similar and showed the signals from FADH$^{\bullet}$, two Fe/S and Mo(V) centres. These signals were simulated individually at 20 and 100 K (Fig. 5) and the EPR parameters found are presented in Tables 2 and 3. The signals obtained are closely related to those observed and described for bovine milk XO and for avian liver XD [39–45]. Both active and desulfo enzymes are reduced simultaneously by dithionite and, accordingly, the Mo(V)

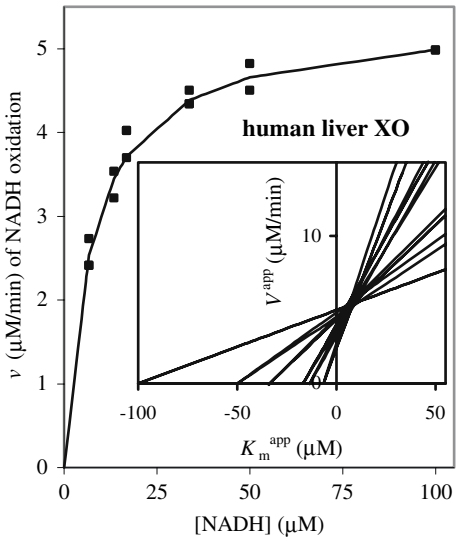

Fig. 2 NADH oxidation catalysed by human liver XO. Initial rates of NADH oxidation, catalysed by human liver XO, were measured spectrophotometrically at 340 nm, in air-equilibrated Tris–HCl 50 mM buffer pH 7.8. The *hyperbolic curve* was generated with the parameters given in Table 1. The apparent kinetics parameters were estimated by the direct linear plot shown in the *inset*

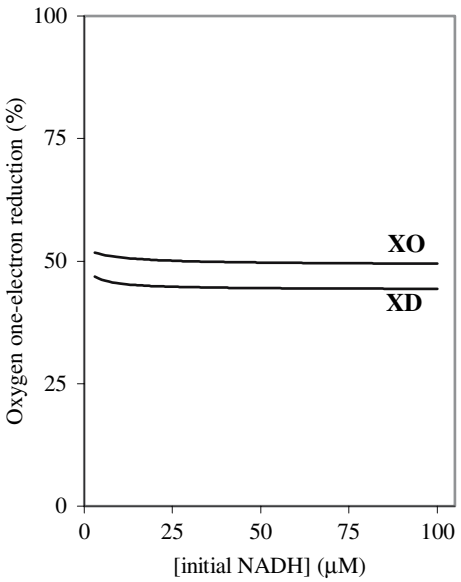

Fig. 3 Percentage of one-electron oxygen reduction, catalysed by both XD and XO forms of rat liver XOR during NADH oxidation. The percentage of one-electron oxygen reduction was calculated to be half of the ratio of the $O_2^{\bullet-}$ formation rate to the NADH oxidation rate, the initial rates calculated from the parameters presented in Table 1

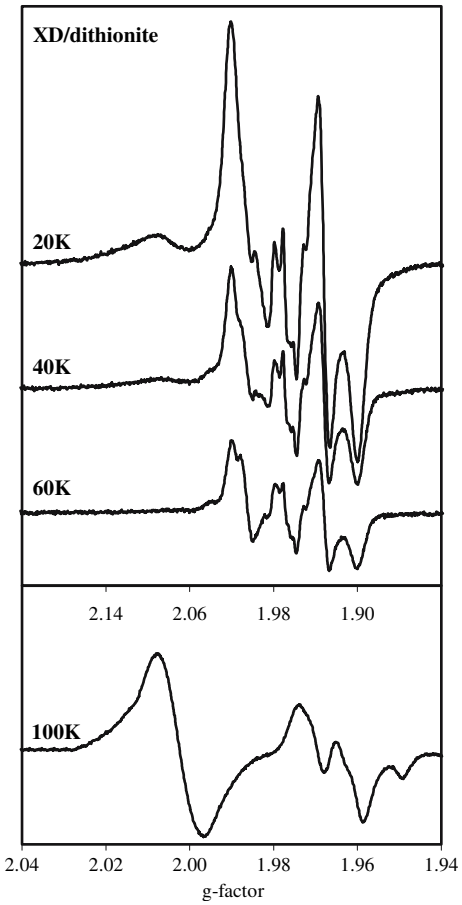

Fig. 4 Electron paramagnetic resonance (*EPR*) spectra of the dithionite-reduced XD form of rat liver XOR. The enzyme (40 nmol) was treated anaerobically with sodium dithionite (400 nmol) for 30 min, and spectra were recorded at the temperatures indicated. Other experimental conditions were as follows: microwave frequency, 9.65 GHz; microwave power, 0.0635 mW; modulation amplitude, 4.05 G; receiver gain, 2.00×10^4

signal was simulated as a mixture of slow and rapid type 1. The isotropic splitting (D = 1.2 mT) of the Mo(V) signals, observed at temperatures of or below 60 K (with or without the Fe/S II reduced), results from the magnetic interaction between the Mo(V) and the Fe/S I centre, as observed by Lowe et al. [46] with bovine milk XO. Also, no interactions were detected between Mo(V) and Fe/S II or between FAD and Mo(V).

Both XD and XO forms of rat liver XOR were also reduced with increasing quantities of NADH. The EPR spectra at 20 and 100 K of NADH-reduced XD (Fig. 6) and XO (not shown) were qualitatively similar to the dithionite-reduced spectra. The EPR signals from NADH-reduced enzymes were simulated individually and the EPR parameters determined are shown in Tables 2 and 3. The simulation of the Mo(V) signal, as a mixture of slow and rapid type-1 signals, was consistent with the known simultaneous reduction by NADH of active and desulfo enzymes, via the flavin (with subsequent reduction of Mo(V) [47]. In addition, the Mo(V) signals were also found to split (D = 1.2 mT) in the presence of the Fe/S I centre (at temperatures below 60 K). The spectra were, however, quantitatively quite different, with the extent of the XD reduction being higher than that of XO. Figure 7 summarises the results of the reductive titration experiments.

The spectra of deflavo-XD in the presence of NADH display no EPR signals (with enzyme-to-NADH molar ratios of 1:500 or less), indicating that the NADH reduction of XD occurs via FAD. In the presence of dithionite, the deflavo enzyme was reduced and the resulting EPR spectra were similar to those of dithionite-reduced XD and XO (Fig. 8), showing the Fe/S centres and Mo(V) signals, but without the flavin signal.

Discussion

NADH oxidase activity of XOR has long been recognised [48–50], but only recently was its potential as a source of ROS realised. Most interest was mainly focused on free-radical metabolism, mediated through hypoxanthine/xanthine oxidation by XO, in biochemical mechanisms associated with a wide variety of human diseases. This ‘‘new’’ ROS-generating pathway, of XOR and NADH, must then be reevaluated in those clinical conditions where an increase in NADH is expected, such as in diseases where hypoxic and reperfusion cycles exist, in ethanol hepatotoxicity and in diabetes [12, 14, 51–54].

To characterise this potential mammalian liver source of ROS, NADH oxidase activity was studied using both XD and XO forms of rat liver XOR. In addition to the fact that mammalian liver enzymes have been poorly studied, other reasons justify the further investigation of liver XOR. The specific activity of human XOR is high in liver and when liver damage occurs, there is an increase in the levels of circulating enzyme, which can bind to vascular endothelium, causing injury [14]. For the diseases referred to above, it seemed more meaningful to carry out studies with liver enzymes than with milk enzymes. Rat liver enzymes, for instance, are kinetically quite different from the human milk enzymes, which show little XOR activity [24], thus hindering comparative studies between xanthine and NADH (physiological reducing substrates) as a ROS source. In addition, a direct comparison between XD and XO forms from the same source can be made. Furthermore, the recently reported XOR-catalysed production of $^{\bullet}$NO, in the presence of nitrite, with either NADH or xanthine as reducing substrates under anaerobic conditions, undoubtedly contributed to further stimulate interest in the physiological and pathological roles of the enzyme. XOR, unlike

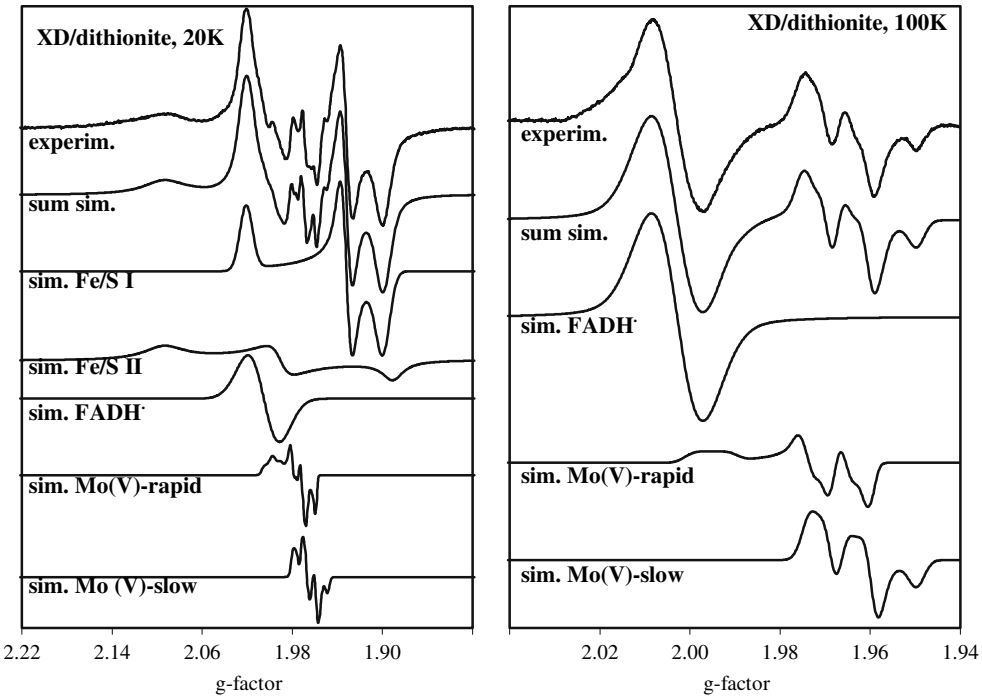

Fig. 5 Simulation of the EPR spectra of the dithionite-reduced XD form of rat liver XOR at 20 and 100 K. Each EPR signal of dithionite-reduced XD, at 20 and 100 K, was simulated individually with the parameters given in Tables 2 and 3. The experimental spectra were recorded with the experimental conditions indicated in Fig. 3

Table 2 Electron paramagnetic resonance (EPR) signal parameters of the Fe/S II, Fe/S I and FADH$^{\bullet}$ from NADH and dithionite-reduced rat liver XD and XO (at 20 K)

Signal	Reducing substrate	Enzyme	g_1[line width (mT)]	g_2[line width (mT)]	g_3[line width (mT)]
Fe/S II	NADH	XD or XO	2.0945 (3.00)	1.9910 (2.50)	1.8895 (2.25)
	Dithionite	XD	2.0945 (4.00)	1.9910 (2.50)	1.8910 (2.50)
	Dithionite	XO	2.1120 (5.50)	1.9910 (4.50)	1.8910 (4.00)
Fe/S I	NADH	XD or XO	2.0210 (1.90)	1.9315 (1.57)	1.8990 (2.375)
	Dithionite	XD	2.0210 (1.90)	1.9320 (1.57)	1.8995 (2.37)
	Dithionite	XO	2.0215 (1.90)	1.9327 (1.57)	1.8987 (2.37)

Signal	Reducing substrate	Enzyme	g[line width (mT)]
FADH$^{\bullet}$	NADH	XD or XO	2.0055 (3.60)
	Dithionite	XD	2.0053 (4.80)
	Dithionite	XO	2.0060 (1.95)

FADH reduced flavin adenine dinucleotide, *g* line width

Table 3 EPR signals parameters of the Mo(V) from NADH and dithionite-reduced rat liver XD and XO (at 20 K)

Signal	Reducing substrate	g_1 [line width (mT)]	g_2 [line width (mT)]	g_3 [line width (mT)]	A_1^H (mT)	A_2^H (mT)	A_3^H (mT)	$D_{1,2,3}$ (mT)
Rapid	NADH	1.9980	1.9723	1.9672	1.000	1.500	1.532	1.200
		(0.65)	(0.45)	(0.35)	0.500			
	Dithionite	1.9980	1.9723	1.9672	1.000	1.500	1.532	1.200
		(0.65)	(0.45)	(0.35)	0.500	0.300	0.250	
Slow	NADH	1.9711	1.9664	1.9557	1.450	1.600	1.400	1.200
		(0.40)	(0.30)	(0.60)				
	Dithionite	1.9719	1.9668	1.9566	1.450	1.600	1.600	1.200
		(0.60)	(0.50)	(0.60)	0.160	0.160	0.160	

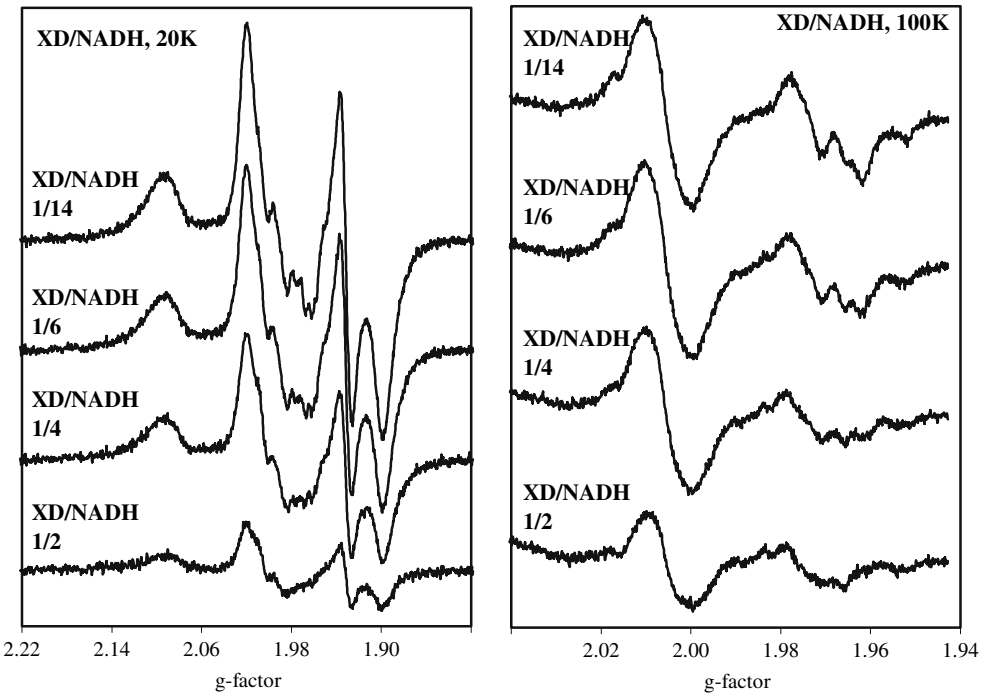

Fig. 6 EPR spectra of the XD form of rat liver XOR reduced with increasing quantities of NADH at 20 and 100 K. The enzyme (40 nmol) was reduced anaerobically, for about 5 min, with NADH, at the XD-to-NADH ratios indicated, and the EPR spectra were recorded at 20 and 100 K. Other experimental conditions were as follows: microwave frequency, 9.65 GHz; microwave power, 0.0635 mW; modulation amplitude, 4.05 G; receiver gain, 2.00×10^5

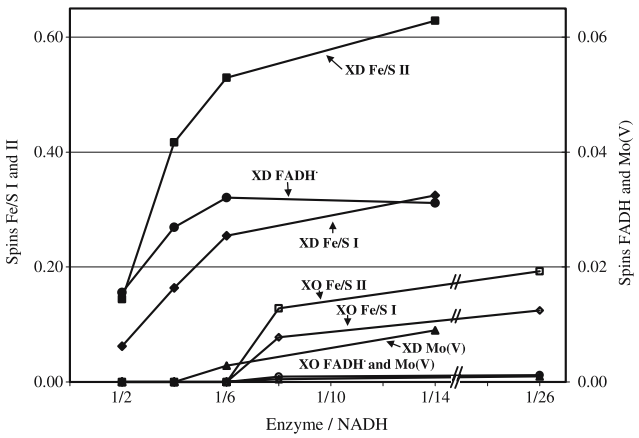

Fig. 7 Anaerobic titration of both XD and XO forms of rat liver XOR with NADH. The enzymes (40 nmol) were reduced anaerobically, for about 5 min, with increasing quantities of NADH, and the EPR spectra were recorded at 20 and 100 K. The FADH$^{\bullet}$, Mo(V) and Fe/S EPR signals were simulated individually (with the parameters given in Tables 2 and 3) and then added together, in different proportions, until good agreement between the simulation sum and the experimental spectrum was observed. Finally, the individual signals were quantified by their areas (double integration of the simulated signal) using a 3 mM Cu^{2+}–EDTA standard. *FADH* reduced flavin adenine dinucleotide

$^{\bullet}$NO synthase, can be an important source of $^{\bullet}$NO in ischaemia, thus promoting the $^{\bullet}$NO-induced vasodilatation [17, 18].

EPR spectra of NADH-reduced XD and XO were quite useful in order to define the spectral parameters of the EPR signals detected for reduced iron–sulfur centres and Mo(V) species. The data make quite clear, as discussed below, that NADH efficiently reduces XD but a large excess of NADH is needed to efficiently reduce XO.

The kinetics studies carried out to compare the NADH oxidation catalysed by the rat liver XD and XO forms of rat liver XOR demonstrated that both enzymes do catalyse NADH oxidation with $O_2^{\bullet-}$ generation. It is, however, significant that the XD form is a better catalyst for NADH oxidation than is the XO form, having a higher specificity constant, whether determined by NADH consumption (8.73 ± 1.36 and 1.07 ± 0.09 μM^{-1} min^{-1}, respectively) or by $O_2^{\bullet-}$ formation (8.40 ± 0.73 and 1.10 ± 0.06 μM^{-1} min^{-1}, respectively).

The percentage of one-electron oxygen reduction catalysed by rat liver XOR was found to be constant as the NADH concentration increased by 50%, indicating that one molecule of $O_2^{\bullet-}$ is formed per NADH molecule. These results are clearly different from those described for xanthine oxidation by XO, where the fraction of $O_2^{\bullet-}$ formed decreases as xanthine concentration increases [8, 9, 56, 57]. Therefore, the chemical equation for the NADH oxidation reaction can be written as

$$2NADH + 3O_2 \rightarrow 2NAD^+ + 2O_2^{\bullet-} + H_2O_2. \quad (1)$$

In addition, it must be emphasised that the kinetics parameters obtained for human liver XO towards NADH oxidation were found to be very similar to those of XO forms of rat liver XOR. Considering the important physiological and pathological roles of human XOR, these re-

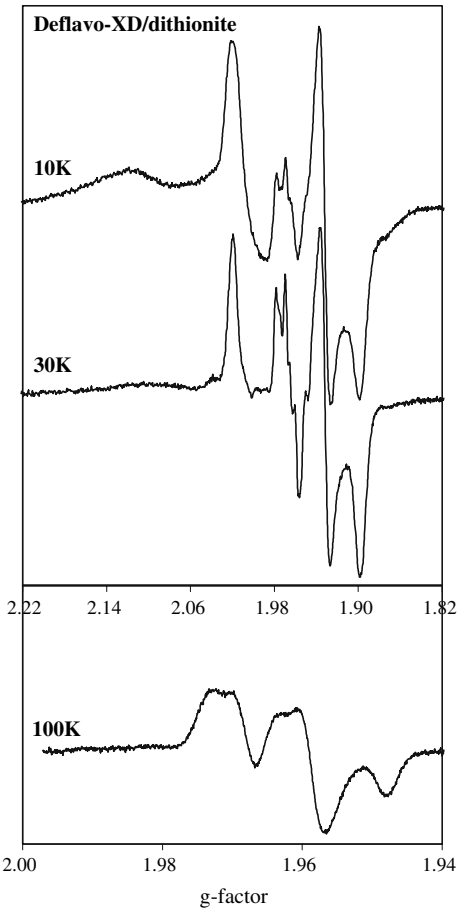

Fig. 8 EPR spectra of the dithionite-reduced deflavo-XD form of rat liver XOR. The enzyme (24 nmol) was treated anaerobically with sodium dithionite (400 nmol) for 30 min, and the spectra were recorded at the temperatures indicated. Other experimental conditions were as follows: microwave frequency, 9.45 GHz; microwave power, 2.01 mW; modulation amplitude, 10.145 G; receiver gain, 2.50×10^4

sults enable us to use rat liver XOR as a first approach in studies whose results are intended to be extrapolated to the human enzyme.

In agreement with the kinetics parameters obtained for both enzyme forms, much higher intensity EPR spectra were observed with NADH-reduced XD than with XO. While FAD removal completely hampers enzyme reduction by NADH (no EPR signals were observed) and abolishes NADH oxidase activity, the kinetics reaction profiles obtained with inactive (desulfo and demolybdo) and allopurinol-inhibited enzymes were identical to those of native enzymes. These results show that the NADH reduction of rat liver XOR occurs via FAD and that alterations at the molybdenum centre do not affect the NADH oxidation kinetics.

With NADH as reducing substrate, the XD form is also more efficient than XO in catalysing the reduction of nitrite to $^{\bullet}$NO [17]. This fact is particularly relevant in vivo, since the XD form is the predominant form in vivo.

Some studies with xanthine as a reducing substrate were carried out (data not shown), and demonstrated that rat liver XD is a better $O_2^{\bullet-}$ source than XO, as previously described [1, 33, 55]. The dehydrogenase form of liver XOR is thus intrinsically more efficient at generating $O_2^{\bullet-}$ than the oxidase form, independently of the reducing substrate. These are remarkable results, in light of the common association of ROS-mediated damage with oxidase enzymes. Therefore, XO is not essential for XOR-catalysed generation of ROS, overcoming the increasingly questioned conversion of XD to XO.

Many pathological conditions arise from free-radical oxidation of DNA, proteins and lipids, and the products of lipid peroxidation; in particular, aldehydes, directly or indirectly, affect many functions integral to cellular homeostasis [58]. Taking into account the ability of XOR to catalyse $O_2^{\bullet-}/H_2O_2$ generation, it is expected that XOR may induce the peroxidation of lipids. In fact, we have shown that rat liver XOR can promote the oxidation of lipids during NADH:O_2 and xanthine:O_2 turnover [59]. In addition, higher peroxidation extents were observed in the presence of NADH, when compared with equimolar concentrations of xanthine, and the rat liver XD form was found to be the most efficient at promoting this oxidative process. Compared with XOR, AO seems to play a minor role in NADH-dependent liposomal lipid damage, which is in agreement with the comparatively low values of the kinetics parameters found for $O_2^{\bullet-}$ formation.

Moreover, a new XOR-dependent route for the generation of peroxynitrite, a strong inflammatory oxidant, was described [19]. Both $^{\bullet}$NO and $O_2^{\bullet-}$ can be produced by XOR, but the efficiency of $ONOO^-$ production depends on the presence or absence of superoxide dismutase and on the rate of $O_2^{\bullet-}$ generation. Our results have shown that the XD form of rat liver XOR is more effective at generating $O_2^{\bullet-}$ than is the XO form. Therefore, following the same reasoning as Godberg et al. [19], in the presence of oxygen, the XD form will have fewer electrons available for the reduction of nitrite than will XO, and it will generate less $ONOO^-$. This condition is more consistent with the likely role of the predominant in vivo XD form in physiological function.

On the whole, we conclude that XOR can be a source of both ROS and reactive nitrogen species, which can induce destructive and useful effects, but the physiological and pathological implications of this complex enzyme are still not completely clarified.

It is worth noting that our results, obtained with rat liver XOR and bovine milk XO, show that enzymes from different sources have different kinetics properties. Nevertheless, the kinetics parameters of human liver XO for NADH oxidation were, indeed, very similar to those of rat liver XO and we believe that these results foresee potential

applications of rat liver enzyme XOR as a model for the human liver enzymes.

References

1. Hille R, Nishino T (1995) FASEB J 9:995–1003
2. Hille R (2005) Arch Biochem Biophys 433:107–116
3. Brondino CD, Romao MJ, Moura I, Moura JJG (2006) Curr Opin Chem Biol 10:109–114
4. Hille R (2006) Eur J Inorg Chem 1913–1926
5. Amaya Y, Yamazaki K, Sato M, Noda K, Nishino T, Nishino T (1990) J Biol Chem 265:14170–14175
6. Nishino T, Nishino T (1997) J Biol Chem 272:29859–29864
7. Enroth C, Eger BT, Okamoto K, Nishino T, Nishino T, Pai E (2000) Proc Natl Acad Sci USA 97:10723–10728
8. Rubbo H, Radi R, Prodanov E (1991) Biochem Biophys Acta 1074:386–391
9. Hausladen A, Fridovich I (1993) Arch Biochem Biophys 304:479–482
10. Suzuki YJ, Forman HJ, Sevanian A (1997) Free Radic Biol Med 22:269–285
11. Babior MB (2000) Am J Med 109:33–44
12. Nishino T, Nakanishi S, Okamoto K, Mizushima J, Hori H, Iwasaki T, Nishino T, Ichimori K, Nakazawa H (1997) Biochem Soc Trans 25:783–786
13. Wright RM, Repine JE (1997) Biochem Soc Trans 25:799–804
14. Harrison R (2002) Free Radic Biol Med 33:774–797
15. Mira L, Maia L, Barreira L, Manso CF (1995) Arch Biochem Biophys 318:53–58
16. Sahinoglu T, Stevens CR, Bhatt B, Blake DR (1996) Methods 9:628–634
17. Godberg BLJ, Doel JJ, Sapkota GP, Blake DR, Stevens CR, Eisenthal R, Harrison R (2000) J Biol Chem 275:7757–7763
18. Li H, Samouilov A, Liu X, Zweier JL (2001) J Biol Chem 276:24482–24489
19. Godberg BLJ, Doel JJ, Durgan J, Eisenthal R, Harrison R (2000) FEBS Lett 475:93–96
20. Palmer R, Ferrige A, Moncada S (1987) Nature 327:524–526
21. Beckman JS, Beckman TW, Chen J, Marshall PA, Freeman BA (1991) Proc Natl Acad Sci USA 87:1620–1624
22. Krenitsky TA, Neil SM, Elion GM, Hitchings GH (1972) Arch Biochem Biophys 150:585–599
23. Komai H, Massey V, Palmer G (1969) J Biol Chem 244:1692–1700
24. Sanders SA, Eisenthal R, Harrison R (1997) Eur J Biochem 245:541–548
25. Williamson JR (1966) J Biol Chem 241:5026–5036
26. Lieber CS (1988) N Engl J Med 319:1639–1650
27. Lieber CS, Savollainem M (1984) Alcohol Clin Exp Res 8:409–423
28. Hille R (1996) Chem Rev 96:2757–2816
29. Waud WR, Rajagopalan KV (1976) Arch Biochem Biophys 172:354–364
30. Maia L, Mira L (2002) Arch Biochem Biophys 400:48–53
31. Saito T, Nishino T (1989) J Biol Chem 264:10015–10022
32. Johson JL, Waud WR, Cohen HJ, Rajagopalan KV (1974) J Biol Chem 249:5056–5061
33. Nishino T, Nishino T, Schopfer LM, Massey V (1989) J Biol Chem 264:2518–2527
34. Harris CM, Massey V (1997) J Biol Chem 272:8370–8379
35. Branzoli U, Massey V (1974) J Biol Chem 249:4339–4345
36. Cornish-Bowden A (1995) Fundamentals of enzyme kinetics. Portland, London
37. Fridovich I (1986) In: Greenwald RA (ed) Handbook of methods for oxygen radical research. CRC, Boca Raton
38. Hille R, Massey V (1985) In: Spiro TG (ed) Molybdenum enzymes. Wiley, New York, pp 443–518
39. Palmer G, Massey V (1969) J Biol Chem 244:2614–2620
40. Bray RC, Vanngard T (1969) Biochem J 114:725–734
41. Hille R, Hagen WR, Dunham WR (1985) J Biol Chem 260:10569–10575
42. Bray RC, Barber MJ, Lowe DJ (1978) Biochem J 171:653–658
43. Gutteridge S, Tanner SJ, Bray RC (1978) Biochem J 175:887–897
44. Barber MJ, Bray RC, Lowe DJ, Coughlan MP (1976) Biochem J 153:297–307
45. Barber MJ, Coughlan MP, Kanda M, Rajagopalan KV (1980) Arch Biochem Biophys 201:468–475
46. Lowe DJ, Lynden-Bell RM, Bray RC (1972) Biochem J 130:239–249
47. Swann JC, Bray RC (1972) Eur J Biochem 26:407–415
48. Murray KN, Chaykin S (1966) J Biol Chem 241:3468–3473
49. Landon EJ, Myles M (1967) Biochem Biophys Acta 143:429–431
50. Massey V, Brumby PE, Komai H, Palmer G (1969) J Biol Chem 244:1682–1691
51. Harrison R (1997) Biochem Soc Trans 25:786–791
52. Wright RM, McManaman JL, Repine JE (1999) Free Radic Biol Med 26:348–354
53. Kato S, Kawase T, Alderman J, Inatomi N, Lieber C (1990) Gastroenterology 98:203–210
54. Chung SSM, Ho ECM, Lam KSL, Chung SK (2003) J Am Soc Nephrol 14:S233–S236
55. Hunt J, Massey V (1992) J Biol Chem 267:21479–21485
56. Fridovich I (1970) J Biol Chem 245:4053–4057
57. Porras AG, Olson JS, Palmer G (1981) J Biol Chem 256:9096–9103
58. Esterbauer H, Zollner H (1989) Free Radic Biol Med 7:197–203
59. Maia L, Vala A, Mira L (2005) Free Radic Res 39:979–986